# Synthesis, Characterization, and Stereocomplex-Induced Gelation of Block Copolymers Prepared by Ring-Opening Polymerization of L(D)-Lactide in the Presence of Poly(ethylene glycol)

**ARTICLE** *in* MACROMOLECULES · SEPTEMBER 2003

Impact Factor: 5.8 · DOI: 10.1021/ma034734i



**2 AUTHORS:**

Su-Ming Li
European Institute of Membranes
**154** PUBLICATIONS **6,984** CITATIONS
SEE PROFILE

Michel Vert
Université de Montpellier
**391** PUBLICATIONS **11,955** CITATIONS
SEE PROFILE

# Synthesis, Characterization, and Stereocomplex-Induced Gelation of Block Copolymers Prepared by Ring-Opening Polymerization of L(D)-Lactide in the Presence of Poly(ethylene glycol)

**Suming Li* and Michel Vert**

*Centre de Recherche sur les Biopolymères Artificiels, Faculté de Pharmacie, 15 Avenue Charles Flahault, 34060 Montpellier, France*

*Received June 2, 2003; Revised Manuscript Received July 22, 2003*

ABSTRACT: A series of block copolymers were synthesized by ring-opening polymerization of L(D)-lactide in the presence of mono- or dihydroxyl poly(ethylene glycol) (PEG) using zinc metal as a catalyst. The resulting diblock and triblock copolymers with relatively short polylactide (PLA) blocks were characterized by various analytical techniques such as $^1$H NMR, SEC, DSC, and X-ray diffraction. The data showed that the copolymers were semicrystalline materials with predominant PEG crystallization although PLA blocks crystallized slightly in some cases. Solubilization tests showed that both the composition and molar mass are determining factors in the water solubility of the copolymers. Bioresorbable hydrogels were prepared from aqueous solutions containing both poly(L-lactide)/PEG and poly(D-lactide)/PEG block copolymers. Hydrogel formation resulted from stereocomplexation occurring between poly(L-lactide) and poly(D-lactide) blocks.

## Introduction

Biodegradable polymers, and especially aliphatic polyesters such as polylactide (PLA), polyglycolide (PGA), and poly(ϵ-caprolactone) (PCL), have been investigated worldwide as biomaterials because of their biocompatibility and biodegradability.[1−3] These polymers present growing interests for temporary therapeutic applications such as sutures, osteosynthetic devices, sustained drug-delivery devices, and scaffolds in tissue engineering.

The delivery of drugs to a human body can be achieved through oral, transdermal, topical, and parenteral administrations. A great deal of work has been done during the past two decades to develop degradable drug-delivery systems (DDS) adapted to these various routes.[1,2] Two types of DDS can be distinguished: implantable and injectable systems. Implantable devices in the form of cylinders, pellets, slabs, disks, and films provide advantages such as prolonged release of drugs, reproducibility of drug-release profiles, ease of fabrication, and so forth.[4−7] However, the implantation of such systems requires surgery with the risk of infection. Injectable systems have been largely investigated in recent years because they circumvent the need for a surgical incision. Among the various injectable drug-delivery systems, micro- or nanoparticles are the most widely investigated because they can be easily introduced into an animal's body by subcutaneous, intramuscular, or intravenous injections.[8−11] However, microparticles can be taken up by lung capillary embolization or by macrophages of the reticuloendothelial system, finally to end up in Kupffer cells in the liver.[1]

Injectable hydrogels are promising substrates for applications in DDS because of their excellent biocompatibility related to the presence of large amounts of water. Bioactive molecules can be physically entrapped in a hydrogel or chemically attached to the polymeric network. Hydrogels are usually formed by a hydrophilic polymer matrix cross linked chemically through covalent bonds or physically through hydrogen bonds, crystallized domains, or hydrophobic interactions.[12]

In a series of papers, Kim et al. reported thermoreversible hydrogels prepared from triblock copolymers containing both poly(ethylene glycol) (PEG) and poly(lactide-co-glycolide) (PLGA) groups.[13−15] A sol−gel transition that depends on the concentration and composition of the copolymers was observed. Hennink et al. prepared a self-assembled hydrogel from enantiomeric PLA oligomers grafted to dextran. The hydrogel was formed from the stereocomplexation of poly(L-lactide) (PLLA) and poly(D-lactide) (PDLA) blocks.[16−18] Later on, Grijpma and Feijen reported the formation of a hydrogel by the stereocomplexation of water-soluble PLLA-PEG-PLLA and PDLA-PEG-PDLA copolymers.[19] Unfortunately, only solubility tests and DSC measurements were performed on the copolymers. Kimura et al. obtained similar hydrogels. However, tetrahydrofuran (THF), which is not acceptable for biomedical applications,[20] was used to dissolve the triblock copolymers.

In a series of papers, we reported on the structure−property relationships and protein-release behaviors of hydrogels of the PLA-PEG-PLA triblock copolymer type.[21−25] Hydrogels were prepared by a phase-separation method consisting of introducing water into a copolymer solution in a biocompatible organic solvent, namely, tetraglycol or poly(ethylene glycol) monotetrahydrofurfuryl ether. PLA blocks constitute cross-linking lipophilic nodes or microdomains in the gel network. These hydrogels are particularly interesting for the release of poorly soluble drugs, proteins, genes, or nucleic acids.

The aim of this work was to obtain bioresorbable hydrogels from aqueous solutions of PLA/PEG copolymers, which should be of great interest to applications in the field of drug delivery or tissue engineering. Copolymers were synthesized by ring-opening polymerization of L(D)-lactide in the presence of PEG with molar masses ranging from 4600 to 20 000, using nontoxic zinc powder as the catalyst. The thus-obtained

* Corresponding author. E-mail: lisuming@univ-montp1.fr.

10.1021/ma034734i CCC: $25.00 
Published on Web 09/27/2003

**Scheme 1. Ring-Opening Polymerization of L(D)-Lactide in the Presence of Dihydroxyl PEG Using Zinc Powder as a Catalyst**

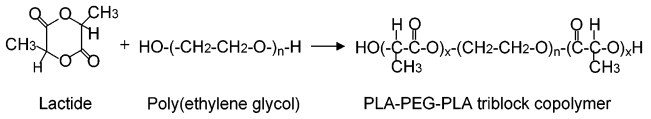


copolymers were characterization by various analytical techniques. Hydrogels were directly prepared from aqueous solutions of PLLA/PEG and PDLA/PEG copolymers. In this article, we report on the synthesis, characterization, and stereocomplex-induced gelation properties of PLA/PEG block copolymers.

## Experimental Section

**Materials.** L-Lactide and D-lactide were obtained from Purac and recrystallized from acetone. Dihydroxyl PEG of various molar masses (4600, 8000, 10 000, 12 000, and 20 000) and a monomethoxy poly(ethylene glycol) (mPEG) with a molar mass of 5000 were supplied by Fluka. Zinc powder was purchased from Merck.

**Polymerization.** Typically, 22 g of PEG and 6 to 12 g of L(D)-lactide were introduced into a flask, the initial molar ratio of ethylene oxide to lactate repeat units (EO/LA) ranging from $^3/_1$ to $^6/_1$. Zinc powder (10 mg) was then added. After degassing, the flask was sealed under vacuum, and the polymerization was allowed to proceed at 140 °C. After 7 days, the product was recovered by dissolution in $CH_2Cl_2$ and precipitation in ether. Finally, the product was dried under reduced pressure up to constant weight.

**Preparation of Hydrogels.** Predetermined amounts of PLLA/PEG and PDLA/PEG copolymers were mixed in 2 mL of distilled water, and the aqueous solutions were centrifuged to yield a homogeneous fluid. Gelation was then allowed to proceed at predetermined temperature for various periods of time.

**Measurements.** $^1$H nuclear magnetic resonance (NMR) spectra were recorded at room temperature with a Bruker spectrometer operating at 250 MHz by using DMSO-$d_6$ as the solvent. Chemical shifts ($\delta$) were given in ppm using tetramethylsilane as an internal reference.

Size-exclusion chromatography (SEC) measurements were performed on a Waters apparatus equipped with an RI detector. THF was used as the mobile phase at a flow rate of 1.0 mL/min. A 1.0% (w/v) solution (20 $\mu$L) was injected for each analysis. Calibration was accomplished with polystyrene standards (Polysciences, Warrington, PA).

Differential scanning calorimetry (DSC) thermograms were registered with a Perkin-Elmer DSC 6 instrument, the heating rate being 10°C/min. Ten milligrams of product was used for each analysis.

X-ray diffraction spectra were registered with a Philips diffractometer composed of a Cu K$\alpha$ ($\lambda$ = 1.54 Å) source, a quartz monochromator, and a goniometric plate.

Raman spectra were recorded with a Jobin-Yvon HG2S spectrometer. The 514.5-nm line of the Spectra Physics 2017 argon laser was used as the excitation source. The laser power was 100 mW. Measurements were performed at room temperature directly on polymer or hydrogel samples without preparation.

Rheological properties were determined on a Carri-Med CSL2 rheometer (TA Instruments). A frequency of 1 Hz and a deformation of 5% were applied.

## Results and Discussion

**Synthesis and Characterization.** Triblock copolymers consisting of a PEG central block and two PLLA or PDLA lateral blocks were synthesized by ring-opening polymerization of L(D)-lactide in the presence of PEG, as shown in Scheme 1. Similarly, PLLA-PEG and PDLA-PEG diblock copolymers were synthesized by using mPEG as an initiator. Nontoxic Zn powder was used as a catalyst instead of stannous octoate or other catalytic systems that are more or less cytotoxic.[26,27] Table 1 presents the various triblock and diblock copolymers prepared in this work.

Triblock copolymers were named using the acronym $L_x$-$EO_y$-$L_x$ or $D_x$-$EO_y$-$D_x$, and diblock copolymers were named as $L_x$-$EO_y$ or $D_x$-$EO_y$. In these acronyms, L, D, and EO represent PLLA, PDLA, and PEG blocks, respectively, $x$ and $y$ representing the number-average degree of polymerization of PLA and PEG blocks. The EO/LA ratio in the copolymers was determined from the integration of NMR resonances belonging to PEG blocks at 3.6 ppm and to PLA blocks at 5.2 ppm as previously described in the literature.[22−25] The number-average molar mass, $\bar{M}_n$, was calculated according to the following equation:

$$\bar{M}_n = \overline{DP}_{PEG} \cdot 44 + \overline{DP}_{PLA} \cdot 72$$

where $\overline{DP}_{PEG} = y = \bar{M}_{nPEG}/44$, $\overline{DP}_{PLA} = nx = \overline{DP}_{PEG}/(EO/LA)$, $n$ is the number of PLA blocks ($n$ = 2 for triblocks and 1 for diblocks), and 44 and 72 are the molar masses of the EO and LA repeat units, respectively.

The EO/LA ratios of the copolymers were higher than the initial ratios according to Table 1. This finding can be assigned to the fact that the conversion of lactide was not complete, unreacted lactide being eliminated by the purification procedure. The largest differences between initial and final EO/LA ratios were found for copolymers initiated by PEG20000. In fact, the higher the molar mass of PEG, the fewer the hydroxyl endgroups or initiation sites and the lower the conversion ratio of lactide under the same reaction conditions.

The water solubility of the copolymers depends not only on the EO/LA ratio but also on the molar mass. In general, a high EO/LA ratio and a low molar mass favor water solubility. For example, PEG4600-initiated triblock copolymers $L_{12}EO_{104}L_{12}$ and $D_{13}EO_{104}D_{13}$ with EO/LA ratios of 4.2 and 4.1 were water soluble, but $L_{24}EO_{104}L_{24}$ and $D_{22}EO_{104}D_{22}$ with EO/LA ratios of 2.2 and 2.4 were not soluble. PEG8000, PEG10000, and PEG12000-initiated copolymers with EO/LA ratios in the range of 4.5 to 7.3 were soluble or formed turbid solutions. PEG20000-initiated $L_{44}EO_{454}L_{44}$ and $D_{46}EO_{454}D_{46}$ with EO/LA ratios of 5.2 and 4.9 were not soluble, in contrast to $L_{21}EO_{454}L_{21}$ and $D_{22}EO_{454}D_{22}$ with EO/LA ratios of 11.0 and 10.5. In the cases of mPEG5000-initiated diblock copolymers, $L_{28}EO_{113}$ and $D_{27}EO_{113}$ with EO/LA ratios of 4.1 and 4.2 were soluble, but $L_{46}EO_{113}$ and $D_{52}EO_{113}$ with EO/LA ratios of 2.5 and 2.2 formed turbid solutions in water.

SEC was performed to evaluate molar mass distributions of the various copolymers. Figure 1 shows the SEC curves of PEG4600 and PEG4600-initiated triblock copolymers $L_{12}EO_{104}L_{12}$ (1L), $D_{13}EO_{104}D_{13}$ (1D), $L_{24}EO_{104}L_{24}$ (2L), and $D_{22}EO_{104}D_{22}$ (2D). The peak of PEG4600 appeared at an elution time of 17.0 min, with a $\bar{M}_n$ of 5300 and a polydispersity index of 1.4. On the SEC curves of the copolymers, the peak corresponding to PEG was not observed, indicating that copolymers were effectively obtained with no residual PEG homopolymer. The molar mass distributions of all of the copolymers were very narrow, with polydispersity indices in the 1.1 to 1.2 range (i.e., less than that of the parent PEG4600). Moreover, the elution time shifted to

**Table 1. PLA/PEG Block Copolymers Obtained by Ring-Opening Polymerization of L(D)-Lactide in the Presence of PEG or MPEG**

| acronym | structure | PEG | lactide | EO/LA[a] | $\overline{DP}_{PEG}$[c] | $\overline{DP}_{PLA}$[d] | $\bar{M}_n$[e] | solubility in water |
|---|---|---|---|---|---|---|---|---|
| 1L | $L_{12}EO_{104}L_{12}$ | PEG4600 | L-lactide | 4.2 (3.0) | 104 | 24 | 6400 | yes |
| 1D | $D_{13}EO_{104}D_{13}$ | PEG4600 | D-lactide | 4.1 (3.0) | 104 | 26 | 6400 | yes |
| 2L | $L_{24}EO_{104}L_{24}$ | PEG4600 | L-lactide | 2.2 (1.5)[b] | 104 | 48 | 8000 | no |
| 2D | $D_{22}EO_{104}D_{22}$ | PEG4600 | D-lactide | 2.4 (1.5) | 104 | 44 | 7700 | no |
| 3L | $L_{20}EO_{182}L_{20}$ | PEG8000 | L-lactide | 4.5 (3.0) | 182 | 40 | 10 900 | yes |
| 3D | $D_{18}EO_{182}D_{18}$ | PEG8000 | D-lactide | 5.0 (3.0) | 182 | 36 | 11 000 | yes |
| 4L | $L_{19}EO_{227}L_{19}$ | PEG10000 | L-lactide | 6.1 (4.0) | 227 | 38 | 12 700 | yes |
| 4D | $D_{20}EO_{227}D_{20}$ | PEG10000 | D-lactide | 5.6 (4.0) | 227 | 40 | 13 700 | yes |
| 5L | $L_{20}EO_{273}L_{20}$ | PEG12000 | L-lactide | 6.8 (4.5) | 273 | 40 | 14 900 | turbid |
| 5D | $D_{19}EO_{273}D_{19}$ | PEG12000 | D-lactide | 7.3 (4.5) | 273 | 38 | 14 700 | turbid |
| 6L | $L_{21}EO_{454}L_{21}$ | PEG20000 | L-lactide | 11.0 (6.0) | 454 | 42 | 23 000 | yes |
| 6D | $D_{22}EO_{454}D_{22}$ | PEG20000 | D-lactide | 10.5 (6.0) | 454 | 44 | 23 100 | yes |
| 7L | $L_{44}EO_{454}L_{44}$ | PEG20000 | L-lactide | 5.2 (3.0) | 454 | 88 | 26 300 | no |
| 7D | $D_{46}EO_{454}D_{46}$ | PEG20000 | D-lactide | 4.9 (3.0) | 454 | 92 | 26 700 | no |
| 8L | $L_{28}EO_{113}$ | mPEG5000 | L-lactide | 4.1 (4.0) | 113 | 28 | 7000 | yes |
| 8D | $D_{27}EO_{113}$ | mPEG5000 | D-lactide | 4.2 (3.0) | 113 | 27 | 6900 | yes |
| 9L | $L_{46}EO_{113}$ | mPEG5000 | L-lactide | 2.5 (2.0) | 113 | 46 | 8300 | turbid |
| 9D | $D_{52}EO_{113}$ | mPEG5000 | D-lactide | 2.2 (2.0) | 113 | 52 | 8700 | turbid |

[a] Calculated from the integration of NMR bands belonging to PEG blocks at 3.6 ppm and to PLA blocks at 5.19 ppm. [b] Data in parentheses corresponding to EO/LA ratios in feed. [c] $\overline{DP}_{PEO} = M_{n\,PEG}/44$. [d] $\overline{DP}_{PLA} = \overline{DP}_{PEO}/(EO/LA)$. [e] $\bar{M}_n = \overline{DP}_{PEG} \cdot 44 + \overline{DP}_{PLA} \cdot 72$.

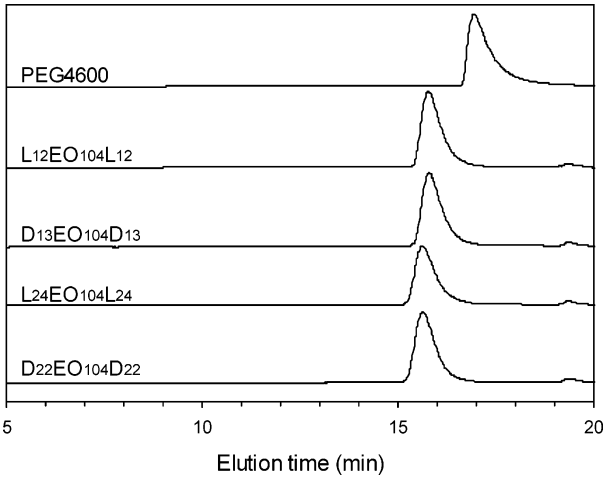


**Figure 1.** SEC curves of PEG4600- and PEG4600-initiated triblock copolymers $L_{12}EO_{104}L_{12}$ (1L), $D_{13}EO_{104}D_{13}$ (1D), $L_{24}EO_{104}L_{24}$ (2L), and $D_{22}EO_{104}D_{22}$ (2D).

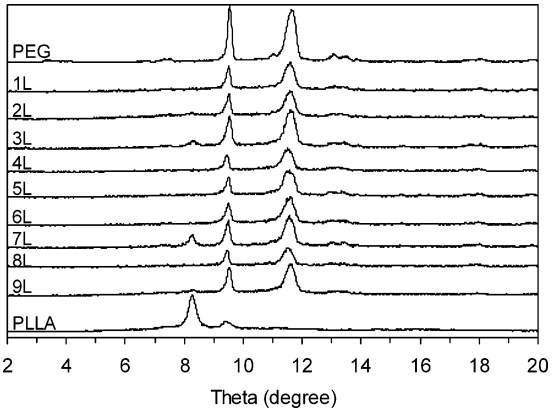


**Figure 2.** X-ray diffraction spectra of PEG, PLLA, and various PLLA/PEG block copolymers.

15.8 for $L_{12}EO_{104}L_{12}$ and $D_{13}EO_{104}D_{13}$ and to 15.6 for $L_{24}EO_{104}L_{24}$ and $D_{22}EO_{104}D_{22}$, with corresponding $\bar{M}_n$ values of 8100, 8200, 9700, and 10100, respectively. Similar features were observed for other copolymers. In the case of higher molar mass copolymers, higher polydispersity indices up to 1.8 were obtained.

Crystalline structures were examined by X-ray diffraction. Figure 2 shows the spectra of various PLLA/PEG block copolymers as well as PLLA and PEG homopolymers in the form of powder. PEG exhibited two main diffraction peaks at 9.7 and 11.8°, and PLLA exhibited an intense peak at 8.3° and a smaller one at 9.4°. The two peaks characteristic of crystalline PEG were detected for all the copolymers, indicating that PEG blocks were able to crystallize although the presence of PLLA blocks disfavored the crystallization of PEG blocks as shown by intensity differences. In contrast, PLLA blocks were not always able to crystallize in the copolymers. PEG4600-initiated 2L showed a very weak peak at 8.5°, indicating a very limited crystallization of PLLA blocks. In contrast, PEG4600-initiated 1L exhibited no PLLA diffraction peaks because of shorter PLLA blocks. In the cases of PEG8000-, PEG10000-, and PEG12000-initiated 3L, 4L, and 5L with similar PLLA block lengths, only PEG8000-initiated 3L exhibited a weak peak at 8.3°. This finding can be explained by the fact that longer PEG blocks disfavored the crystallization of PLLA blocks more than shorter ones. Similarly, PEG20000-initiated 7L showed a relatively intense peak at 8.3°, and 6L showed no PLLA diffraction peak because of a shorter PLLA block length. In the case of mPEG5000-initiated 8L and 9L diblock copolymers, only 9L with longer PLLA blocks showed a very small PLLA diffraction peak. Similar features were obtained for PDLA/PEG copolymers whose structures were very close to those of PLLA/PEG copolymers.

Figure 3a shows DSC thermograms of PEG4600 and PEG4600-initiated $L_{12}EO_{104}L_{12}$ (1L) and $L_{24}EO_{104}L_{24}$ (2L) triblock copolymers. PEG4600 exhibited a melting temperature of $T_m = 67.5$ °C and a melting enthalpy of $\Delta H_m = 170.8$ J/g. In contrast, $T_m$ and $\Delta H_m$ of copolymer 1L decreased to 55.7 °C and 96.7 J/g, respectively. In the case of copolymer 2L containing longer PLLA blocks, $T_m$ and $\Delta H_m$ further decreased to 50.9 °C and 67.2 J/g. These data confirmed that the presence of PLLA blocks disfavored the crystalization of PEG. The longer the PLLA block length, the lower the degree of crystallinity of PEG as reflected by the $\Delta H_m$ values. After the first heating, the samples in the molten state were immersed in liquid nitrogen, and a second heating was then

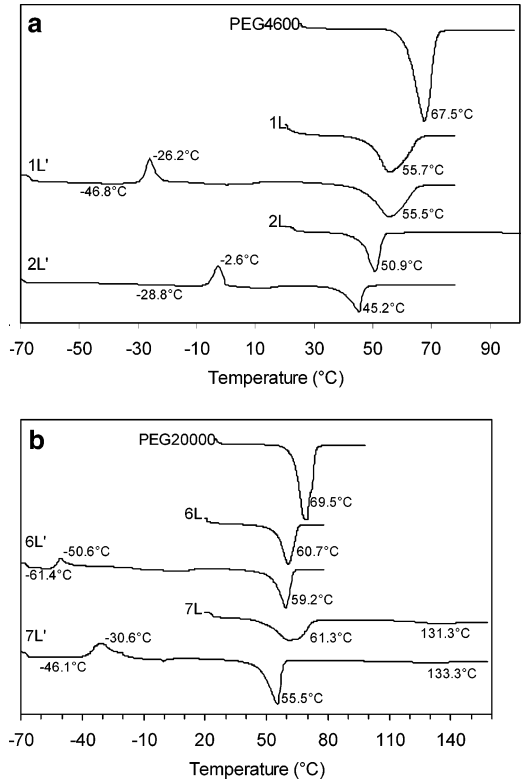


**Figure 3.** (a) DSC thermograms of PEG4600 and PEG4600-initiated triblock copolymers $L_{12}EO_{104}L_{12}$ (2L) and $L_{24}EO_{104}L_{24}$ (2L), 1L′ and 2L′ (second heating after quenching). (b) DSC thermograms of PEG20000 and PEG20000-initiated triblock copolymers $L_{21}EO_{454}L_{21}$ (6L) and $L_{44}EO_{454}L_{44}$ (7L), 6L′ and 7L′ (second heating after quenching).

performed on quenched samples to determine the glass-transition ($T_g$) and crystallization ($T_c$) temperatures. No $T_g$ was detected for PEG4600 because it crystallized too fast. In contrast, both $T_g$ and $T_c$ were observed in the case of the copolymers whose crystallizability was reduced by the presence of PLLA blocks. Copolymer 1L exhibited a glass transition at −46.8 °C and a crystallization peak at −26.2 °C, and 2L showed a $T_g$ at −28.8 °C and a $T_c$ at −2.6 °C. It is known that the $T_g$ of PEG is about −65 °C and the $T_g$ of PLLA is in the range of 50 to 60 °C. Therefore, $T_g$ values of the copolymers were between those of PEG and PLLA, closer to PEG than to PLLA, which indicates that PEG and PLA are partially miscible in the amorphous state. Moreover, the longer the PLLA block, the higher the $T_g$ of the copolymer. Similar trends were found for 1D and 2D copolymers.

Figure 3b shows DSC thermograms of PEG20000- and PEG20000-initiated $L_{21}EO_{454}L_{21}$ (6L) and $L_{44}EO_{454}L_{44}$ (7L) triblock copolymers. Similar trends were found as in the cases of 1L and 2L. Table 2 presents the thermal properties of the various PEGs and copolymers. All of the PEGs and mPEG showed similar $T_m$ values, with corresponding $\Delta H_m$ values in the 160 to 180 J/g range. In the case of the copolymers, PEG8000-initiated 3L, PEG20000-initiated 7L and 7D, and mPEG5000-initiated 9L and 9D exhibited a small melting peak in the 109 to 149 °C range. This second melting peak was assigned to PLA crystallites, in agreement with X-ray diffraction data in the cases of 3L, 7L, and 9L showing a peak at 8.3° characteristic of PLA crystallization.

**Table 2. Thermal Properties of PLA/PEG Block Copolymers Obtained by Ring-Opening Polymerization of L(D)-Lactide in the Presence of PEG or MPEG**

| acronym | $T_m$(°C)[a] | $\Delta H$(J/g)[a] | $T_g$[b] | $T_c$[b] |
|---|---|---|---|---|
| PEG4600 | 67.5 | 170.8 | | |
| 1L | 55.7 | 96.7 | −46.8 | −26.2 |
| 1D | 54.2 | 97.8 | −47.1 | −32.5 |
| 2L | 50.9 | 67.2 | −28.8 | −2.6 |
| 2D | 54.6 | 74.2 | −35.8 | −5.5 |
| PEG8000 | 68.0 | 172.7 | | |
| 3L | 61.2 (149.0) | 77.9 (0.7) | −50.1 | −36.6 |
| 3D | 61.8 | 105.6 | −52.5 | −42.2 |
| PEG10000 | 69.7 | 163.9 | | |
| 4L | 62.1 | 112.5 | −57.5 | −42.9 |
| 4D | 60.4 | 105.5 | −57.9 | −43.6 |
| PEG12000 | 69.1 | 163.4 | | |
| 5L | 61.6 | 111.6 | −58.8 | −46.0 |
| 5D | 60.8 | 120.7 | −59.7 | −47.0 |
| PEG20000 | 69.5 | 160.5 | | |
| 6L | 60.7 | 99.4 | −61.4 | −50.6 |
| 6D | 59.9 | 111.0 | −62.2 | −50.3 |
| 7L | 61.3 (131.3) | 76.9 (8.2) | −46.1 | −30.6 |
| 7D | 63.9 (129.0) | 75.1 (4.1) | −50.6 | −34.6 |
| mPEG5000 | 68.5 | 179.9 | | |
| 8L | 58.6 | 91.2 | −49.8 | −36.3 |
| 8D | 59.4 | 83.0 | −57.8 | −40.9 |
| 9L | 57.6 (109.0) | 86 (0.7) | −38.8 | −19.9 |
| 9D | 55.8 (122.0) | 62 (6.2) | −33.3 | −14.2 |

[a] Obtained from the first heating. [b] Obtained from the second heating.

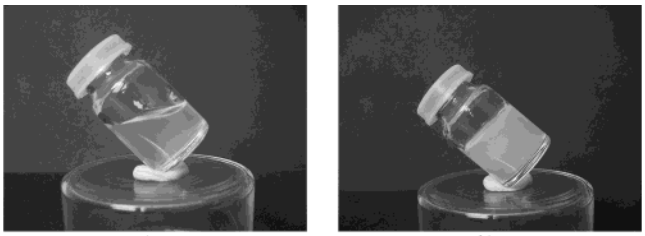


**Figure 4.** (a) Aqueous solution (20%) of $L_{12}EO_{104}L_{12}$ and (b) a hydrogel formed by a 20% solution containing both $L_{12}EO_{104}L_{12}$ and $D_{13}EO_{104}D_{13}$ after 2 days at 25 °C.

**Hydrogel Properties.** Stereocomplexation is a well-known phenomenon for optically active PLA stereocopolymers.[28−34] A stereocomplex can be obtained from the coprecipitation of PLLA and PDLA in solution[28,29] or through cooling from a melt of both polymers.[30] An oligomeric stereocomplex was also obtained during the in vitro degradation of poly(DL-lactide) because of the presence of isotactic L and D sequences along polymer chains.[31,32] Once released by degradation, these sequences are prone to regroup and form an oligomeric stereocomplex. In the case of enantiomeric PLA-PEG-PLA copolymers, a stereocomplex was obtained by coprecipitation or solution casting from homogeneous solutions.[33,34]

When PLLA/PEG is mixed with PDLA/PEG in an aqueous solution, interactions between L and D blocks can lead to stereocomplexation and to the formation of a hydrogel. Figure 4 shows comparatively a 20% aqueous solution of $L_{12}EO_{104}L_{12}$ and a hydrogel formed by a 20% solution containing both $L_{12}EO_{104}L_{12}$ and $D_{13}EO_{104}D_{13}$. Both were initially viscous and transparent solutions. The $L_{12}EO_{104}L_{12}$ solution remained unchanged at 25 °C. In contrast, the solution containing both $L_{12}EO_{104}L_{12}$ and $D_{13}EO_{104}D_{13}$ became more and more viscous and whitish, in agreement with the occurrence of L/D interactions and stereocomplexation. After 48 h at 25°C, the solution did not flow anymore,

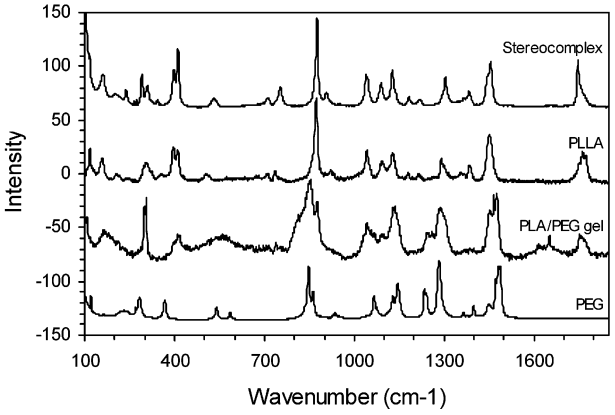


**Figure 5.** Raman spectra of a stereocomplex formed by the coprecipitation of PLLA and PDLA, semicrystalline PLLA, a hydrogel formed by a 15% solution containing both $L_{20}EO_{182}L_{20}$ and $D_{18}EO_{182}D_{18}$, and PEG8000.

indicating the formation of a hydrogel. Hydrogels were obtained from aqueous solutions of all soluble PLLA/PEG and PDLA/PEG block copolymers by varying gelation conditions such as temperature, time, and concentration. In the cases of $L_{20}EO_{273}L_{20}$ and $D_{19}EO_{273}D_{19}$ as well as $L_{46}EO_{113}$ and $D_{52}EO_{113}$, which formed turbid solutions in water, hydrogels were formed at 37 °C.

The formation of a stereocomplex within the hydrogels was confirmed by Raman spectroscopy, a noninvasive technique that is sensitive to morphology modifications. Figure 5 shows comparatively the Raman spectra of a stereocomplex formed by the coprecipitation of PLLA and PDLA, semicrystalline PLLA, a hydrogel formed by a 15% solution containing both $L_{20}EO_{182}L_{20}$ and $D_{18}EO_{182}D_{18}$, and PEG8000. Spectral differences were observed between PLLA and the stereocomplex because of different helical conformations as reported in the literature.[28] The cell dimensions of PLLA α-form crystals are $a = 1.07$ nm, $b = 0.595$ nm, and $c = 2.78$ nm, the crystal system being pseudo-orthorhombic. Each unit cell contains two left-handed $10_3$ helices. In the case of the stereocomplex, the crystal system is triclinic with the following cell dimensions: $a = 0.916$ nm, $b = 0.916$ nm, $c = 0.870$ nm, $\alpha = 109.2°$, $\beta = 109.2°$, and $\gamma = 109.8°$. Each unit cell contains a PLLA chain and a PDLA chain that are packed in parallel in a $3_1$ helical conformation.[28] For the sake of clarity, three regions with no or little PEG contribution are selected on the Raman spectra and are shown in Figure 6 (320 to 470, 700 to 1000, and 1700 to 1850 $cm^{-1}$).

In the 320 to 470 $cm^{-1}$ range, two sharp bands at 411 and 398 $cm^{-1}$ were observed for the stereocomplex, the band at 411 $cm^{-1}$ being more intense than the band at 398 $cm^{-1}$. They are assigned to $\delta$CCO deformations. The two bands were also observed for semicrystalline PLLA, but the band at 411 $cm^{-1}$ appeared slightly less intense than the band at 398 $cm^{-1}$. In the case of the hydrogel, two weak bands were distinguished, the intensity difference between them being similar to that of the stereocomplex. The weakness of the bands resulted from the low PLA content and high water content of the hydrogel. In the 700 to 1000 $cm^{-1}$ range, an intense band was detecetd at 876 $cm^{-1}$ for the stereocomplex, which was assigned to $\nu$C−COO stretching. The band appeared at 873 $cm^{-1}$ for PLLA. The hydrogel presented a band at 877 $cm^{-1}$ similar to that of the stereocomplex and a broad one at 855 $cm^{-1}$ belonging to a PEG component, PEG8000, showing two sharp bands at 848 and 863 $cm^{-1}$. Finally, in the 1700 to 1850 $cm^{-1}$ range, the stereocomplex showed a single band at 1746 $cm^{-1}$ with a broad diffusion band, which was assigned to $\nu$C═O stretching. In contrast, PLLA exhibited three bands at 1748, 1762, and 1773 $cm^{-1}$. Concerning the hydrogel, a weak band was observed at 1750 $cm^{-1}$ with a broad diffusion band, which resembled that of the stereocomplex. All of these results showed that stereocomplexation occurred between L and D blocks within the hydrogel. X-ray diffraction spectra on the lyophilized hydrogels also confirmed the presence of a stereocomplex.

Hydrogel formation was confirmed by rheological measurements. Figure 7 shows the evolution of both storage and loss moduli of a 15% hydrogel composed of $L_{20}EO_{182}L_{20}$ and $D_{18}EO_{182}D_{18}$. Gelation was achieved for 24 h at 37 °C. The storage modulus ($G'$) was largely superior to the loss modulus ($G''$) and remained almost constant at 20 °C as a function of time (Figure 7a), indicating that it was effectively a hydrogel. In the case of viscous solutions, $G'$ is lower than $G''$. When the temperature increased from 20 to 37 °C at 1 °C/min (Figure 7b), both $G'$ and $G''$ decreased, $G'$ decreasing faster than $G''$. However, $G'$ remained higher than $G''$. These results showed that the cross-link density decreased with increasing temperature. In fact, the hydrogel was a dynamic system. It can be assumed that

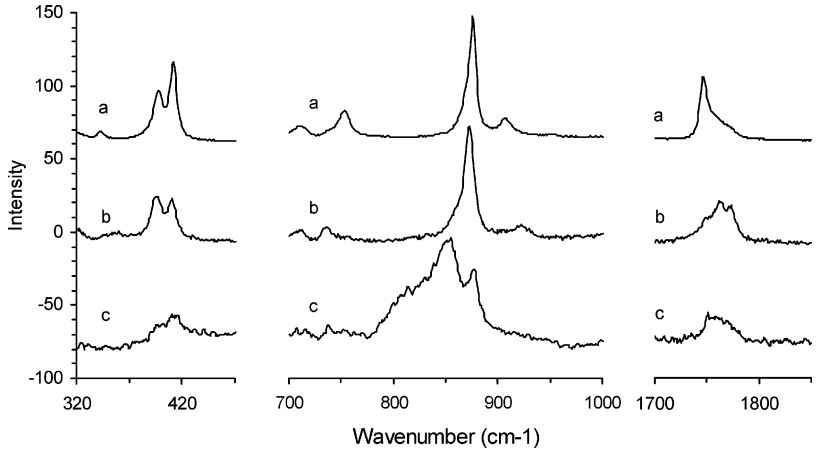


**Figure 6.** Selected regions of Raman spectra (320 to 470, 700 to 1000, and 1700 to 1850 $cm^{-1}$): (a) stereocomplex formed by the coprecipitation of PLLA and PDLA, (b) semicrystalline PLLA, and (c) a hydrogel formed by a 15% solution containing both $L_{20}EO_{182}L_{20}$ and $D_{18}EO_{182}D_{18}$.

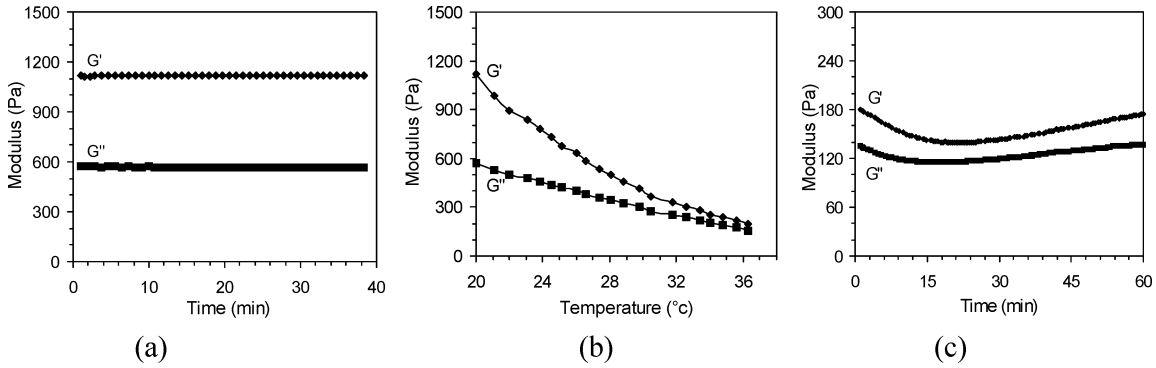


**Figure 7.** Storage modulus ($G'$) and loss modulus ($G''$) evolutions of a 15% hydrogel containing $L_{20}EO_{182}L_{20}$ and $D_{18}EO_{182}D_{18}$ after 24 h at 37 °C: (a) at 20 °C as a function of time, (b) from 20 to 37 °C at 1 °C/min, and (c) at 37 °C as a function of time.

L/D interactions and stereocomplexation constitute an equilibrium, the latter contributing much more to cross linking than the former. At higher temperature, the stereocomplex becomes less stable, and the equilibrium tends to simple L/D interactions, leading to a modulus decrease. Scanning at 37 °C as a function of time showed that both moduli decreased at first and then increased (Figure 7c). The increase in the moduli can be assigned to the fact that at 37 °C stereocomplexation between L and D blocks continued, the hydrogel becoming more and more consistent.

It is of interest to compare these hydrogels with those derived from PEG-PLGA-PEG copolymers.[13−15] In the latter case, the aqueous polymer solution was initially a free-flowing solution, and a sol−gel transition could be observed around body temperature. The mechanism of this transition was assigned to a micellar expansion accompanying an increase in aggregation driven by hydrophobic forces. Unfortunately, no rheological studies were reported on these PEG-PLGA-PEG hydrogels, and the sol−gel transition was determined by a test tube-inverting method.[13−15] In the case of hydrogels prepared from aqueous solutions containing both PLLA/PEG and PDLA/PEG copolymers, gelation is induced by stereocomplexation between PLLA and PDLA blocks and is thus time- and temperature-dependent. Gelation is faster at 37 than at 20 °C. Moreover, the length of the PLA blocks plays an important role in the gelation process. Hennink et al. reported that the $\overline{DP}$ of PLA blocks should be at least 11 to obtain a hydrogel from PLA-grafted dextran,[16] and blends of PLLA and PDLA oligomers can form a stereocomplex with a $\overline{DP}$ higher than 7.[36] In the case of PLA/PEG copolymers, $L_{12}EO_{104}L_{12}$ exhibited the lowest $\overline{DP}$ of PLA blocks.

Therefore, an injectable drug-delivery system can be designed because of the bioresorbability and thermosensitivity of these hydrogels. This system presents several advantages with respect to most drug-delivery systems. First, the synthesis of polymers requires only one step, in contrast to PEG-PLGA-PEG systems whose synthesis requires two steps.[13−15] Second, the formulation is very simple without an organic solvent, in contrast to microparticulate systems[1] and in situ-forming implants.[37] Third, the hydrogel is easily injectable. In situ gelation is also possible because hydrogels can be formed at 37 °C. Last but not least, the system is totally bioresorbable, in contrast to thermosensitive hydrogels derived from *N*-isopropylacrylamide or poloxamers that are more or less toxic and nonbiodegradable.[38,39] Therefore, this work strongly supports the use of these bioresorbable hydrogels formed by stereocomplexation for the sustained delivery of bioactive molecules, in particular, high molar mass proteins or other biopolymers.

## Conclusions

PLA/PEG block copolymers were prepared by ring-opening polymerization of L(D)-lactide using nontoxic zinc metal as a catalyst. Most of the resulting diblock and triblock copolymers were soluble in water because PLA blocks were relatively short. The water solubility of the copolymers depended on both the composition and the molar mass. The copolymers were semicrystalline materials, with PEG blocks crystallizing in all cases. Bioresorbable hydrogels were prepared from aqueous solutions containing both PLLA/PEG and PDLA/PEG block copolymers. Hydrogel formation resulted from stereocomplexation occurring between PLLA and PDLA blocks. These hydrogels should be of great interest as substrates for the sustained delivery of bioactive molecules.

**Acknowledgment.** We are indebted to Dr. G. Kister for Raman spectra recording and to Dr. A. El Ghzaoui for rheological measurements.

## References and Notes

(1) Li, S.; Vert, M. In *The Encyclopedia of Controlled Drug Delivery*; Mathiowitz, E., Ed.; Wiley & Sons: New York, 1999; p 71.
(2) Dunn, R. L. In *Biomedical Applications of Synthetic Biodegradable Polymers*; Hollinger, J. O., Ed.; CRC Press: Boca Raton, FL, 1995; p 17.
(3) Li, S. *J. Biomed. Mater. Res.* **1999**, *48*, 342−353.
(4) Pitt, C. G.; Gratzl, M. M.; Himmel, G. L.; Surles, J.; Schindler, A. *Biomaterials* **1981**, *2*, 215−220.
(5) Kaetsu, I.; Yoshida, M.; Asano, M.; Yamanaka, H.; Imai, K.; Yuasa, H.; Mashimo, T.; Susuki, K.; Katakai, R.; Oya, M. *J. Controlled Release* **1987**, *6*, 249−263.
(6) Fitzgerald, J. F.; Corrigan, O. I. *J. Controlled Release* **1996**, *42*, 125−132.
(7) Schakenraad, J. M.; Oosterbaan, J. A.; Nieuwenhuis, P.; Molenaar, I.; Olijslager, J.; Potman, W.; Eenink, M. J. D.; Feijen, J. *Biomaterials* **1988**, *9*, 116−120.
(8) Sanders, L. M.; Kent, J. S.; McRae, G. I.; Vickery, B. H.; Tice, T. M.; Lewis, D. H. *J. Pharm. Sci.* **1984**, *73*, 1294−1297.
(9) Arshady, R. *J. Bioact. Compat. Polym.* **1990**, *5*, 315−342.
(10) Kyo, M.; Hyon, S. H.; Ikada, Y. *J. Controlled Release* **1995**, *35*, 73−77.
(11) Takada, S.; Uda, Y.; Toguchi, H.; Ogawa, Y. *J. Pharm. Sci. Technol.* **1995**, *49*, 180−184.
(12) Hoffman, A. S. *Adv. Drug Delivery Rev.* **2002**, *54*, 3−12.
(13) Jeong, B.; Bae, Y. H.; Lee, D. S.; Kim, S. W. *Nature* **1997**, *388*, 860−862.
(14) Jeong, B.; Bae, Y. H.; Kim, S. W. *J. Controlled Release* **2000**, *63*, 155−163.

(15) Jeong, B.; Kim, S. W.; Bae, Y. H. *Adv. Drug Delivery Rev.* **2002**, *54*, 37−51.
(16) de Jong, S. J.; De Smedt, S. C.; Wahls, M. W. C.; Demeester, J.; Kettenes-van den Bosch, J. J.; Hennink, W. E. *Macromolecules* **2000**, *33*, 3680−3686.
(17) de Jong, S. J.; van Eerdenbrugh, B.; van Nostrum, C. F.; Kettenes-van den Bosch, J. J.; Hennink, W. E. *J. Controlled Release* **2001**, *71*, 261−275.
(18) de Jong, S. J.; De Smedt, S. C.; Demeester, J.; van Nostrum, C. F.; Kettenes-van den Bosch, J. J.; Hennink, W. E. *J. Controlled Release* **2001**, *72*, 47−56.
(19) Grijpma, D. W.; Feijen, J. *J. Controlled Release* **2001**, *72*, 247−249.
(20) Fujiwara, T.; Mukose, T.; Yamaoka, T.; Yamane, H.; Sakurai, S.; Kimura, Y. *Macromol. Biosci.* **2001**, *1*, 204−208.
(21) Vert, M.; Li, S.; Rashkov, I.; Espartero, J. L. French Patent 95 14144, 1995.
(22) Rashkov, I.; Manolova, N.; Li, S.; Espartero, J. L.; Vert, M. *Macromolecules* **1996**, *29*, 50−56.
(23) Li, S.; Rashkov, I.; Espartero, J. L.; Manolova, N.; Vert, M. *Macromolecules* **1996**, *29*, 57−62.
(24) Li, S.; Anjard, S.; Rashkov, I.; Vert, M. *Polymer* **1998**, *39*, 5421−5430.
(25) Molina, I.; Li, S.; Bueno Martinez, M.; Vert, M. *Biomaterials* **2001**, *22*, 363−369.
(26) Schwach, G.; Coudane, C.; Engel, R.; Vert, M. *Polym. Bull.* **1994**, *32*, 617−623.
(27) Tanzi, M. C.; Verderio, P.; Lampugnani, M. G.; Resnati, M.; Dejana, E.; Sturani, E. *J. Mater. Sci.: Mater. Med.* **1994**, *5*, 393−396.
(28) Okihara, T.; Tsuji, M.; Kawagushi, A.; Katayama, K.-I.; Tsuji, H.; Hyon, S.-H.; Ikada, Y. *J. Macromol. Sci., Phys.* **1991**, *30*, 119−140.
(29) Tsuji, H.; Hyon, S.-H.; Ikada, Y. *Macromolecules* **1992**, *25*, 2940−2946.
(30) Tsuji, H.; Ikada, Y. *Macromolecules* **1993**, *26*, 6918−6926.
(31) Li, S.; Vert, M. *Polym. Int.* **1994**, *33*, 37−41.
(32) Li, S.; Girod-Holland, S.; Vert, M. *J. Controlled Release* **1996**, *40*, 41−53.
(33) Stevels, W. M.; Ankone, M. J. K.; Dijkstra, P. J.; Feijen, J. *Macromol. Chem. Phys.* **1995**, *11*, 3687−3694.
(34) Lim, D. W.; Park, T. G. *J. Appl. Polym. Sci.* **2000**, *75*, 1615−1623.
(35) Kister, G.; Cassanas, G.; Vert, M. *Polymer* **1998**, *39*, 267−273.
(36) de Jong, S. J.; van Dijk-Wolthuis, N. E.; Kettenes-van den Bosch, J. J.; Schuyl, P. J. W.; Hennink, W. E. *Macromolecules* **1998**, *31*, 6397−6402.
(37) Hatefi, A.; Amsden, B. *J. Controlled Release* **2002**, *80*, 9−15.
(38) Chen, G. H.; Hoffman, A. S. *Nature* **1995**, *373*, 49−52.
(39) Malstom, M.; Lindman, B. *Macromolecules* **1992**, *25*, 5446−5450.

MA034734I